Environmental Science & Technology

Article

pubs.acs.org/est

Estimation of Aerosol Mass Scattering Efficiencies under High Mass Loading: Case Study for the Megacity of Shanghai, China

Zhen Cheng,[†,⊥] Jingkun Jiang,*[,†,‡] Changhong Chen,[§] Jian Gao,[∥] Shuxiao Wang,*[,†,‡] John G. Watson,[#,▽] Hongli Wang,[§] Jianguo Deng,[†] Buying Wang,[†] Min Zhou,[§] Judith C. Chow,[#,▽] Marc L. Pitchford,[#] and Jiming Hao[†,‡]

[†]School of Environment, State Key Joint Laboratory of Environment Simulation and Pollution Control, Tsinghua University, Beijing 100084, China

[‡]State Environmental Protection Key Laboratory of Sources and Control of Air Pollution Complex, Beijing 100084, China

[§]State Environmental Protection Key Laboratory of the Formation and Prevention of Urban Air Pollution Complex, Shanghai Academy of Environmental Sciences, Shanghai 200233, China

[∥]Chinese Research Academy of Environmental Science, Beijing 100012, China

[⊥]School of Environmental Science and Engineering, Shanghai Jiao Tong University, Shanghai 200240, China

[#]Division of Atmospheric Sciences, Desert Research Institute, 2215 Raggio Parkway, Reno, Nevada 89512, United States

[▽]SKLLQG, Institute of Earth Environment, Chinese Academy of Sciences, Xi'an, 710075, China

ABSTRACT: Aerosol mass scattering efficiency (MSE), used for the scattering coefficient apportionment of aerosol species, is often studied under the condition of low aerosol mass loading in developed countries. Severe pollution episodes with high particle concentration frequently happened in eastern urban China in recent years. Based on synchronous measurement of aerosol physical, chemical, and optical properties at the megacity of Shanghai for two months during autumn 2012, we studied MSE characteristics at high aerosol mass loading. Their relationships with mass concentrations and size distributions were examined. It was found that MSE values from the original US IMPROVE algorithm could not represent the actual aerosol characteristics in eastern China. It results in an underestimation of the measured ambient scattering coefficient by 36%. MSE values in Shanghai were estimated to be 3.5 ± 0.55 m^2/g for ammonia sulfate, 4.3 ± 0.63 m^2/g for ammonia nitrate, and 4.5 ± 0.73 m^2/g for organic matter, respectively. MSEs for three components increased rapidly with increasing mass concentration in low aerosol mass loading, then kept at a stable level after a threshold mass concentration of 12−24 $\mu g/m^3$. During severe pollution episodes, particle growth from an initial peak diameter of 200−300 nm to a peak diameter of 500−600 nm accounts for the rapid increase in MSEs at high aerosol mass loading, that is, particle diameter becomes closer to the wavelength of visible lights. This study provides insights of aerosol scattering properties at high aerosol concentrations and implies the necessity of MSE localization for extinction apportionment, especially for the polluted regions.

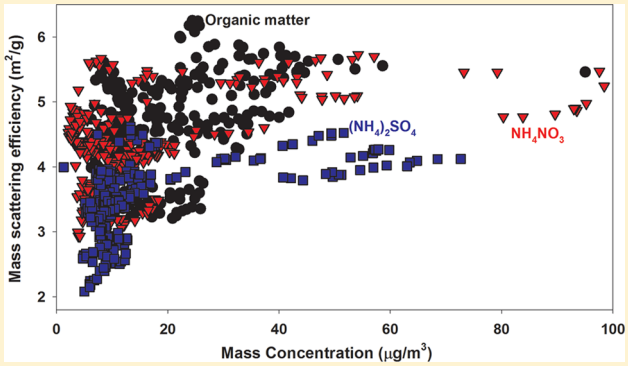

INTRODUCTION

Fine particulate matter ($PM_{2.5}$) has adverse impacts on human health through deposition at the respiratory organs[1−3] and exhibits optical extinction effects such as visibility degradation and climate change.[4−6] Aerosol extinction effects are due to their scattering and absorption of light. Aerosol mass scattering efficiency (MSE) is a key index that link $PM_{2.5}$ mass concentration and its scattering coefficient. Knowing MSEs for different aerosol components is important in haze pollution apportionment and in estimating radiative forcing using climate models.[7,8]

The average MSEs of global reported measurements from 1990 to 2007 is 2.5 ± 0.6 m^2/g for sulfate, 2.7 ± 0.5 m^2/g for nitrate and 3.9 ± 1.5 m^2/g for organic matter in fine mode.[9] The notable variation range is mainly due to the differences in aerosol morphology, physic-chemical properties, and mixing state.[9] Widely used MSEs are those from the "IMPROVE" (Interagency Monitoring of Protected Visual Environments) program,[5,10,11] which is derived from long-term measurements in U.S. national parks. Due to its simplicity and practicality, the IMPROVE algorithm is also used in places outside the U.S., for example, the megacities of Guangzhou,[12−14] Xi'an,[15] Tianjin,[16]

Received: September 19, 2014
Revised: December 14, 2014
Accepted: December 15, 2014
Published: December 15, 2014

DOI: 10.1021/es504567q
Environ. Sci. Technol. 2015, 49, 831−838

Table 1. Measured Indices, Time Resolution, And Instruments Used in the Field Campaign

measurement index	instrument (manufacturer)	time resolution	uncertainties
$PM_{2.5}$ inorganic species (SO_4^{2-}, NO_3^-, NH_4^+, Cl^-)	MARGA ADI 2080 (Applikon Analytical, The Netherlands)	1 h	20%[a]
$PM_{2.5}$ organic species (OC, EC)	RT4 carbon analyzer (Sunset Laboratory, Inc., OR)	30 min	OC:18%[a] EC:31%[a]
$PM_{2.5}$ and PM_{10} mass concentrations (40 °C heating)	FH62 C-14 β-ray (Thermo Scientific Co., MA)	5 min	22%[a]
particle size distribution (Dry, 3 nm-10 μm)	Nano SMPS & SMPS & APS 3321 (TSI Inc., MN)	5 min	
aerosol scattering coefficient (RH $\leq$ 60%, 525 nm)	Aurora 3000 Nephelometer (EcoTech Pty Ltd., Australia)	5 min	3%[b]
species size distribution (0.18−18 μm in eight bins for ions and carbon)	MOUDI Model 100 (MSP Co., MN)	24 h every 2 days	
$PM_{2.5}$ chemical species (elements, ions, carbon)	Partisol 2300 Speciation Sampler (Thermo Scientific Corp., MA)	24 h	
Ambient RH	Met One Station (Met One Co., OR)	5 min	3%[c]

[a]Relative differences comparing with offline $PM_{2.5}$ sampling and analysis results. [b]Relative differences comparing with a collocated TSI 3563 nephelometer. [c]Provided by the instrument manufacturer.

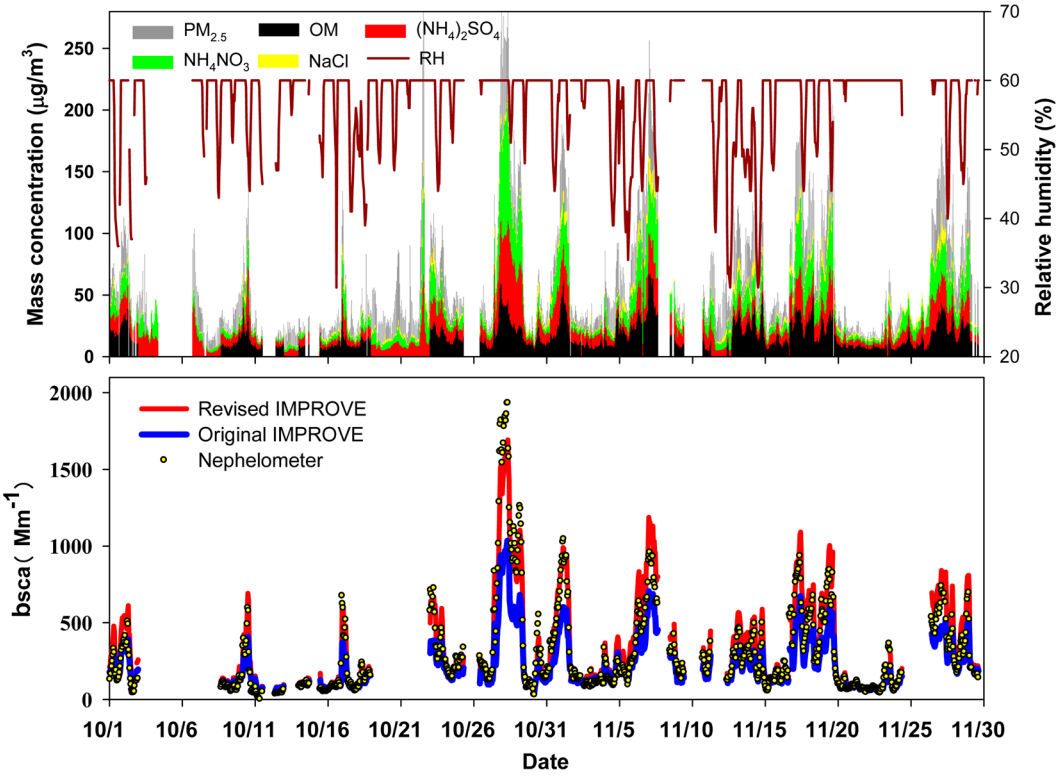

Figure 1. Temporal variation of aerosol mass concentration and scattering coefficient (bsca) calculated by IMPROVE algorithms and measured values by the nephelometer (RH $\leq$ 60%).

and Nanjing[17] in China. However, the IMPROVE MSEs were measured in rural areas with natural-dominant impact and relative low aerosol mass loading. The variation of MSEs under high aerosol loading caused by the anthropogenic emission can be different. Furthermore, the reported MSE values are usually episode-average or season-average based on the offline aerosol sampling data sets,[9,11,18] resulting in the incapacity of observing dynamic variation of MSEs with high temporal resolution during pollution episodes.

China is undergoing rapid industrialization and urbanization, and the observed ambient aerosol loading is much higher than that of U.S. and Europe, both for integrated mass level and major composition concentration.[19,20] The high mass level during pollution episodes in China, as well as the advances of online instruments for aerosol physical, chemical, and optical properties, provide the opportunities for investigating the high-resolution variation of MSEs under high mass loading.

In this study, a two-month field campaign was conducted during a severe $PM_{2.5}$ pollution season in Shanghai, one of the largest megacities in China with the coal consumption of 43.2 million tons of standard coal equivalent and the vehicle population of 3.0 million in 2010.[21] Its annual average $PM_{2.5}$ concentration was 60.7 $\mu g/m^3$ in 2013, 6 times the guideline value of 10 $\mu g/m^3$ suggested by the World Health Organization.[22] The applicability of MSEs from the IMPROVE algorithm was evaluated. Local hourly MSEs for three major scattering species (ammonia sulfate, ammonia nitrate, and organic matter) were estimated based on observation data and Mie theory. Their relations with aerosol mass concentrations and size distributions over a large mass range were investigated.

MATERIALS AND METHODS

Field Campaign. The observation site was located at Shanghai Academy of Environmental Sciences (121.25°E, 31.10°N).

DOI: 10.1021/es504567q
Environ. Sci. Technol. 2015, 49, 831−838

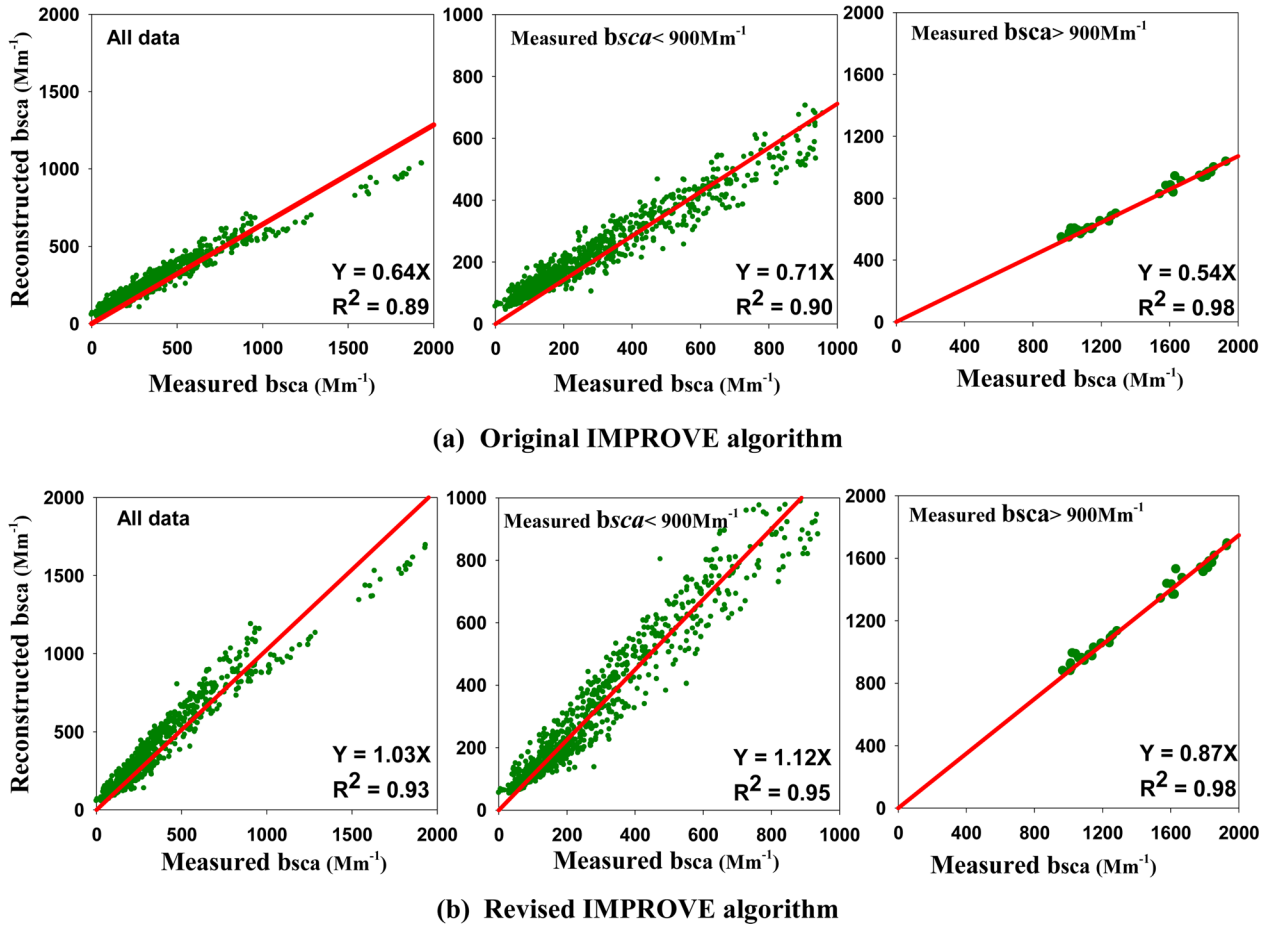

Figure 2. Linear regression between calculated aerosol scattering coefficients (bsca) by IMPROVE algorithms and measured values by the nephelometer (RH ≤ 60%).

There were no major industrial sources nearby. The sampling height was 15 m above ground level. The observation campaign covered two months of autumn 2012, that is, from October 10, 2012 to November 30, 2012. Previous studies in Shanghai reported that severe PM pollution episodes frequently occurred during autumn.[23,24] As summarized in Table 1, aerosol mass concentration, size distributions, water-soluble ions, carbonaceous species, ambient relative humidity (RH), and scattering coefficient were measured. $PM_{2.5}$ and PM_{10} mass concentrations were measured by a β-ray apparatus with 5 min resolution. Dry particle size distributions from 3 nm to 10 μm were measured by a home-built spectrometer including two scanning mobility particle sizers (SMPS) and one aerodynamic particle sizer (APS) with 5 min resolution.[25] $PM_{2.5}$ water-soluble ions included SO_4^{2-}, NO_3^-, NH_4^+, and Cl^- were measured in situ using a Monitor for Aerosols and Gases in Ambient Air (MARGA) with 1-h resolution.[26] $PM_{2.5}$ organic carbon (OC) and elemental carbon (EC) were measured by a semi-continuous OC-EC field analyzer with 30 min resolution.[27] Aerosol scattering coefficient was measured by an integrated nephelometer with internal RH below 60%. Ambient RH was measured by a Met One Station with 5 min resolution. All the above online measurement results were then averaged to 1 h resolution.

Segregated aerosol offline samples with eight size bins (0.18−18 μm) were collected by aluminum foil substrates in a micro-orifice uniform-deposit impactor (MOUDI)[28] with continuous 24 h operation every 2 days, and followed by the analysis of water-soluble ions and organic carbons.[29,30] $PM_{2.5}$ offline samples were collected by Teflon and quartz glass filters in a Partisol 2300 speciation sampler with daily resolution, followed by trace element analysis using an Epsilon 5 ED-X-ray Fluorescence,[15] water-soluble ions and organic carbons.[29] QA/QC was practiced for the field campaign, including routine calibration and maintenance for online instruments and offline samplers. Laboratory chemical analysis was carried out following standard operating procedures, as reported in another paper.[29] In addition, in situ measured concentrations of $PM_{2.5}$ components were compared with those from offline $PM_{2.5}$ sampling. The Aurora nephelometer results were compared with a collocated TSI 3563 nephelometer. Relative differences are given in Table 1. Considering that different sampling and analytical methods were used, the uncertainty ranges are reasonable and acceptable.

Evaluation of IMPROVE Algorithms. Hourly concentrations of ammonia sulfate, ammonia nitrate, and sea salt of $PM_{2.5}$ were estimated by multiplying MARGA reported sulfate, nitrate, and chloride concentrations by a factor of 1.375, 1.29, and 1.8, respectively. Hourly organic matter concentration was estimated by multiplying the Sunset Carbon Analyzer reported OC concentrations by a local measured factor of 1.55.[31] Hourly coarse PM concentration was the differences between PM_{10} and $PM_{2.5}$ concentrations. Hourly soil concentration was reconstructed uniformly using measured element concentrations (Al, Si, Ca, Fe, Ti) from daily sampling for each day.[8] Considering the scattering hygroscopicity of the measured particles inside the nephelometer, the minimum value between

DOI: 10.1021/es504567q
Environ. Sci. Technol. 2015, 49, 831−838

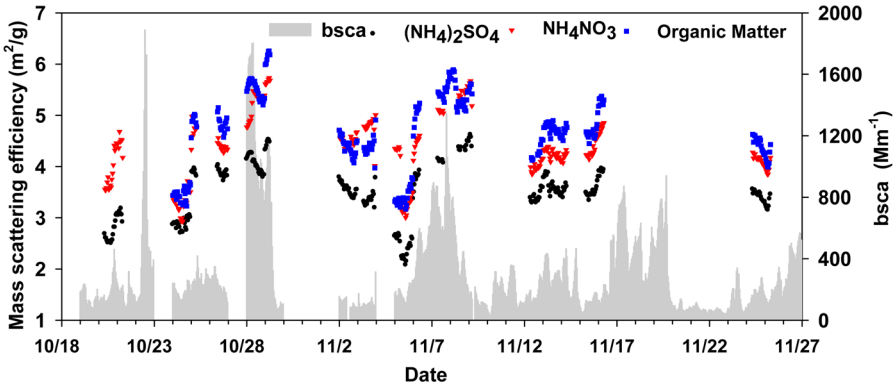

Figure 3. Temporal variation of mass scattering efficiencies for three $PM_{2.5}$ species and measured aerosol scattering coefficient (bsca) (RH ≤ 60%).

Table 2. Mass Scattering Efficiencies Found in Different Studies

species	method	location	MSE value (m^2/g)	reference
ammonia sulfate	theoretical	Shanghai	3.5 (min: 2.1, max: 4.7)	this study
	IMPROVE_O[a]	U.S. rural	3	Watson et al.[5]
	IMPROVE_R[b]	U.S. rural	2.2 (SM[c]); 4.8 (LM[d])	Pitchford et al.[10]
	Theoretical	review	2.1	Hand and Malm[9]
	MLR[e]	review	2.8	Hand and Malm[9]
	MLR[e]	Mediterranean	2.66	Sciare et al.[38]
	MLR[e]	Guangzhou	2.9(spring); 2.5(summer); 4.8(autumn); 5.3(winter)	Tao et al.[18]
	MLR[e]	Guangzhou	2.2 (SM[c]); 3.2 (LM[d])	Jung et al.[14]
ammonia nitrate	theoretical	Shanghai	4.3 (Min: 2.4, Max: 5.8)	this study
	IMPROVE_O[a]	U.S. rural	3	Watson et al.[5]
	IMPROVE_R[b]	U.S. rural	2.4 (SM[c]); 5.1 (LM[d])	Pitchford et al.[10]
	MLR[e]	review	2.8	Hand and Malm[9]
	MLR[e]	Guangzhou	3.2(spring); 2.6(summer); 4.9(autumn); 5.5(winter)	Tao et al.[18]
	MLR[e]	Guangzhou	2.4 (SM[c]); 4.5 (LM[d])	Jung et al.[14]
organic matter	theoretical	Shanghai	4.5 (Min: 3.2, Max: 6.3)	this study
	IMPROVE_O[a]	U.S. rural	4	Watson et al.[5]
	IMPROVE_R[b]	U.S. rural	2.8 (SM[c]); 6.1 (LM[d])	Pitchford et al.[10]
	Theoretical	review	2.6 (SM[c]); 5.6 (LM[d])	Hand and Malm[9]
	MLR[e]	review	3.1	Hand and Malm[9]
	MLR[e]	Mediterranean	4.2	Sciare et al.[38]
	MLR[e]	Guangzhou	3.3(spring); 2.8(summer); 5.1(autumn); 6.2(winter)	Tao et al.[18]
	MLR[e]	Guangzhou	2.8 (SM[c]); 4.9 (LM[d])	Jung et al.[14]

[a]Original IMPROVE algorithm. [b]Revised IMPROVE algorithm. [c]Small mode. [d]Large mode. [e]Multiple linear regression.

ambient relative humidity (RH) and the internal threshold value of 60% was used for the input RH of hygroscopic curves in original and revised IMPROVE algorithms. Since no dust storm was observed during the field campaign, the angular truncation errors of the nephelometer was corrected by multiplying an empirical factor of 1.073 at 550 nm.[32] Finally, the hourly aerosol species concentrations and RH were input into the original and revised IMPROVE algorithms to obtain aerosol scattering coefficients, which were then compared with the measured scattering coefficients by the nephelometer.

Calculation of MSEs for Aerosol Species. The scattering efficiency (Q_{sca}) for single spherical particle of a given aerosol species (index j) was calculated using Mie theory by inputting the particle diameter (D_p), refractive index (n_j), and incident wavelength (λ).[33,34] The MSE value for species j at the size of D_p with a given particle density (ρ_j) was estimated using eq 1.[9] The wavelength was selected as 525 nm and the refractive index and density for ammonia sulfate, ammonia nitrate, and organic matter was derived from Pitchford et al.[10]

$$\mathrm{MSE}(j, D_p) = 3Q_{sca}(n_j, D_{bin}, \lambda)/(2\rho_j D_{bin}) \quad (1)$$

For inhomogeneous particles with different sizes, the integrated $PM_{2.5}$ MSE for species j was estimated by weighting the MSE value for different sizes with mass concentration size distribution ratio ($C_{j,Dbin}$) for particles below 2.5 μm (as shown in eq 2).

$$\mathrm{MSE}(j, \mathrm{PM}_{2.5}) = \sum_{\mathrm{bin}=1}^{D_{bin}\le 2.5\mu m} \mathrm{MSE}(j, D_{bin}) C_{j,Dbin} / \sum_{\mathrm{bin}=1}^{D_{bin}\le 2.5\mu m} C_{j,Dbin} \quad (2)$$

Assuming different aerosol species were externally mixed, aerosol species mass concentration size distribution ratio was derived by coupling MOUDI daily data sets with hourly particle size distribution data sets as suggested by Quinn et al.[35] First, the daily volume ratio of different aerosol species for individual

DOI: 10.1021/es504567q
Environ. Sci. Technol. 2015, 49, 831−838

MOUDI size bin was derived from MOUDI daily species mass concentration with specific species density. Secondary, the daily volume ratio was used to split the integrated number concentration of PSD into different aerosol species for the covered PSD size bins and corresponding hours by keeping 1 h time resolution. Finally, the number concentration of individual species for each PSD size bin was converted to mass concentration by the specific species density which will then be for MSE calculation.

RESULTS AND DISCUSSION

Bias Estimation of IMPROVE Algorithm. Hourly aerosol scattering coefficients estimated by the original and revised IMPROVE algorithms and measured by the nephelometer are shown in Figure 1. Temporal trends of the scattering coefficient during the whole observation period are consistent among three methods. The agreement among three data sets are good when the measured aerosol scattering coefficient is lower than 300 Mm^{-1}, which usually occurs at low aerosol mass concentrations. When the measured scattering coefficient is higher than 300 Mm^{-1}, predictions by the original IMPROVE algorithm are 34% lower than the measured scattering coefficients, while predictions by the revised IMPROVE algorithm are only 7% higher than the measured values. Underestimation by the original IMPROVE algorithm is as high as 38−45% during heavy pollution episodes, e.g., those occurred in October. 28, November 1, 7, and 17−19.

Quantitative deviations between the measured scattering coefficients and predictions by IMPROVE algorithms were estimated. Figure 2 presents the linear regression results between them under three conditions, that is, overall average, measured scattering coefficient higher and lower than 900 Mm^{-1}. A strong linear relationship was observed between measurement data and predictions, that is, the R^2 values are 0.89 and 0.93 for the original and revised IMPROVE algorithms, respectively. For the original algorithm, however, prediction is lower than the measured coefficient by 36% when fitting all the data. The deviation increases to 46% when only fitting data under scattering coefficient greater than 900 Mm^{-1}. The performance of the revised IMPROVE algorithm is better than the original algorithm. 3% overestimation is observed when fitting all measurement data. This bias is a 12% overestimation at low scattering coefficient range and a 13% underestimation at high scattering coefficient range.

Studies in another Chinese megacity of Guangzhou reported similar deviations, that is, the original algorithm underestimates the reconstructed scattering coefficient at high aerosol loadings and the revised algorithm overestimates it at low aerosol loadings.[14,18,36] For data from U.S. monitoring sites, however, both the orginal one and the revised one underpredict during high aerosol loadings and overpredict during low aerosol loadings. The underestimation and overestimation ratios reported by different studies are 11−26% and 25−54%, respectively.[10,11,37] The revised IMPROVE algorithm could reduce the integrated bias at two extreme ends in general.[10]

Major differences between the original and revised algorithms are the MSE values of ammonia sulfate, ammonia nitrate, and organic matter.[10] In the original algorithm, these MSEs are constant under the whole mass range. In the revised algorithm, the MSEs are settled for two modes (i.e., small mode with the mean diameter of 200 nm and large mode with the mean diameter of 500 nm). Higher MSE values are used in the large mode than those in the small mode).[10] The higher the measured species mass concentration, the higher percentage will be distributed into the large mode by the cutoff concentration of 20 $\mu g/m^3$. To understand the different performances of IMPROVE algorithms in Chinese megacities versus in U.S. monitoring sites, it is needed to evaluate local MSEs in China.

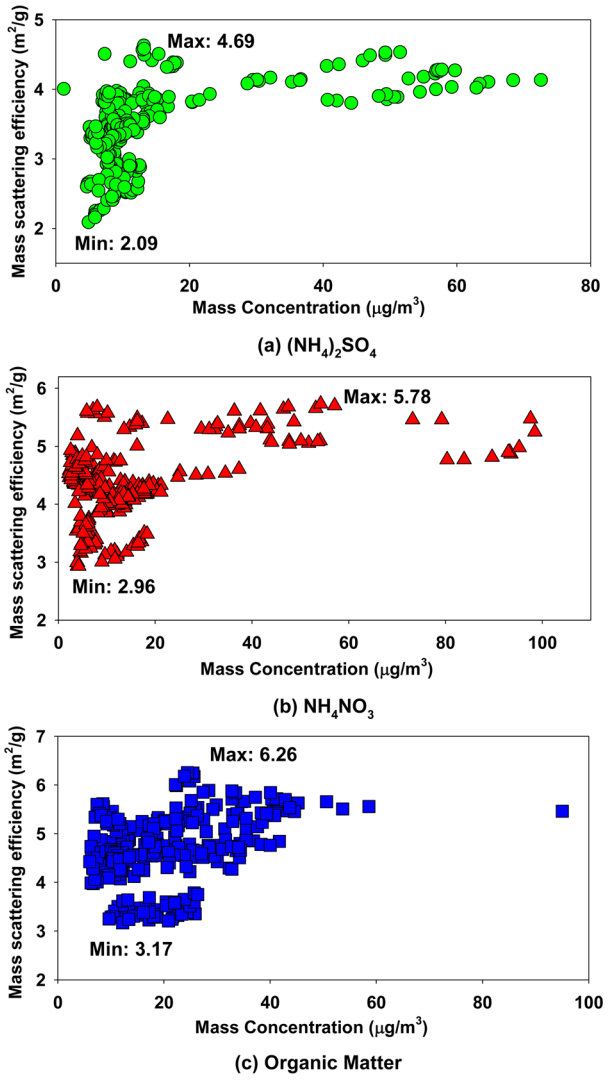

Figure 4. Mass scattering efficiencies versus mass concentration for three $PM_{2.5}$ species: (a) ammonia sulfate, (b) ammonia nitrate, and (c) organic matter.

Local MSEs for Major $PM_{2.5}$ Scattering Species. Figure 3 shows the temporal variations of calculated local hourly MSEs for three major $PM_{2.5}$ scattering species, that is, ammonium sulfate, ammonium nitrate, and organic matter. The total number of hourly MSEs is 300−350 for each species. During the observation period, the average MSEs in Shanghai are 3.5 ± 0.55 m^2/g for ammonium sulfate, 4.3 ± 0.63 m^2/g for ammonium nitrate, and 4.5 ± 0.73 m^2/g for organic matter, respectively. The temporal variation trends are similar for three aerosol species. Their MSEs increase rapidly during the formation of a pollution episode, and decrease rapidly with the scavenging of the episode. These trends are particularly notable for the two severe pollution episodes on October 28 and November 7. The hourly MSEs reach as high as 4.7 m^2/g for ammonium sulfate, 5.8 m^2/g for ammonium nitrate, and 6.3 m^2/g for organic matter, and as low as 2.1 m^2/g for ammonium sulfate, 2.4 m^2/g for ammonium nitrate, and 3.2 m^2/g for organic matter during these two episodes.

DOI: 10.1021/es504567q
Environ. Sci. Technol. 2015, 49, 831−838

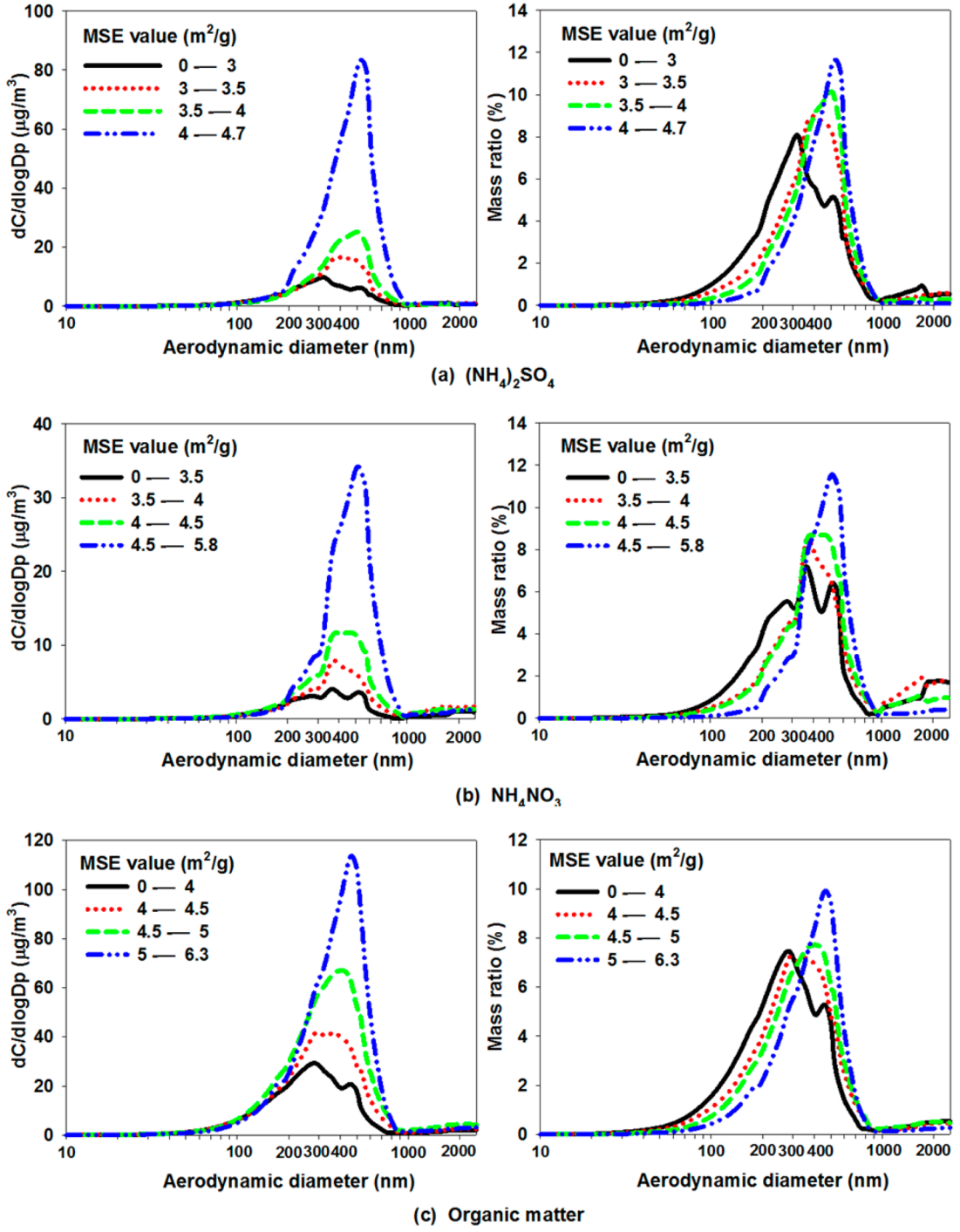

Figure 5. Size distribution of mass concentration and mass ratio under different mass scattering efficiency (MSE) groups for three $PM_{2.5}$ species: (a) ammonia sulfate, (b) ammonia nitrate, and (c) organic matter. The line type and color together represents different groups of MSE value.

Meanwhile, the MSEs do not increase proportionally with the pollution extent. For the episode on October 28, the average scattering coefficient is 1213 Mm^{-1}, 2.3 times that of the episode on November 7. However, the corresponding average MSEs for the two episodes are similar, that is, 4.13 and 4.19 m^2/g for ammonium sulfate, 5.31 and 5.18 m^2/g for ammonium nitrate, 5.64 and 5.33 m^2/g for organic matter, respectively. The variation of MSEs during pollution episodes emphasizes the need for online high temporal resolution MSE evaluation when apportioning each component contribution to the total extinction coefficient, which becomes feasible recently with the rapid development of aerosol mass spectrometry and other online analytical methods.

Table 2 summarizes MSEs estimated by this study and those reported previously. The MSEs in the original IMPROVE algorithm is 3 m^2/g for ammonium sulfate and ammonium nitrate, 4 m^2/g for organic matter. The corresponding values of this study are 3.5, 4.3, and 4.5 m^2/g, higher by 17%, 43%, and 13%, respectively. This explains the underestimation in aerosol scattering coefficients when applying the original algorithm in Shanghai (as discussed in the previous section). The MSEs for the two modes in the revised IMPROVE algorithm are

DOI: 10.1021/es504567q
Environ. Sci. Technol. 2015, 49, 831−838

2.2 and 4.8 m^2/g for ammonium sulfate, 2.4 and 5.1 m^2/g for ammonium nitrate, 2.8 and 6.1 m^2/g for organic matter, which is comparable to the observed minimum and maximum values in this study, namely 2.1 and 4.7 m^2/g for ammonium sulfate, 2.4 and 5.8 m^2/g for ammonium nitrate, 3.2 and 6.3 m^2/g for organic matter. This explains the better agreement between the revised algorithm and measured data for the polluted periods.

Hand and Malm[9] summarized MSEs reported by different studies from 1990 to 2007 which estimated MSEs using Mie theory and multiple linear regression (MLR). Sciare et al.[38] investigated the MSEs for ammonium sulfate and organic matter for a Mediterranean city using MLR method. Comparing to these MSEs found in the developed area with low aerosol mass loadings, the MSEs for all three species found in this study are 25−54% higher. Tao et al.[18] reported that in the megacity of Guangzhou, China, the MSEs in polluted winter season are 2.1−2.2 times higher than those in summer season (typically with low aerosol mass loading). Their reported MSEs for winter season are comparable with what we found in Shanghai during this study. The MSEs for the large mode reported by Jung et al.[14] are 12−33% lower than those in the revised IMPROVE algorithm and the maximum MSEs found in this study, mostly because their observation was made in the summer season.

Relationship between MSEs and Species Mass Concentrations. As shown previously, MSEs of major scattering species vary in a large range during each pollution episode. Since MSE for individual species is influenced by its mass ratio size distribution, the notable change of MSE during a pollution episode indicates that aerosol properties change dramatically. Figure 4 presents hourly MSEs as a function of species mass concentrations. Similar patterns are observed for all three scattering species, that is, MSE increases rapidly with increasing species mass concentration in the low concentration range, then slowly reaches a plateau. Specifically, MSE for ammonium sulfate increases from 2.09 m^2/g to 4.69 m^2/g when ammonium sulfate concentration is below 15 $\mu g/m^3$. It then fluctuates in a narrow range at higher ammonium sulfate concentration. MSE for ammonium nitrate increases from 2.96 m^2/g to 5.69 m^2/g when ammonium nitrate concentration is lower than 12 $\mu g/m^3$. It then fluctuates in a narrow range when further increasing ammonium nitrate concentration. For organic matter, its minimum mass concentration (6.2 $\mu g/m^3$) is not low enough to see the rapid increase in MSE. It reaches the maximum of 6.3 m^2/g at 24 $\mu g/m^3$, then fluctuates around 5.6 m^2/g when organic matter concentration is higher than 24 $\mu g/m^3$.

To further understand the above trend, the relationship between MSE and mass concentration size distribution was investigated. The mass ratio size distribution is calculated based on mass concentration size distribution. Figure 5 presents mass concentration and mass ratio size distributions under different MSE groups for these three species. MSEs were divided into four groups with the step size of 0.5 m^2/g and the starting value of 3 m^2/g for ammonia sulfate, 4 m^2/g for ammonia nitrate, and 4.5 m^2/g for organic matter, respectively. Figure 5 indicates that higher MSEs correspond to not only higher mass concentration, but also higher peak diameters for both mass concentration and mass ratio size distributions, that is, the peak diameter increases from 200−300 nm to 500−600 nm. Calculation using Mie theory shows that maximum MSEs for aerosol species with monodisperse size to scatter visible light with the wavelength of 550 nm usually occur at the geometric diameter of 500−600 nm,[39] which means the more adjacent to this range for mass ratio size distribution, the higher MSEs for the integrated $PM_{2.5}$ species. With increasing species mass concentration, the peak diameters of three scattering species grow toward the more efficient scattering diameter range and results in an increase in the integrated MSEs. Two known mechanisms might drive the growth of peak diameter from 200−300 nm to 500−600 nm with the mass concentration increase. For ammonia sulfate and nitrate, the higher ion concentrations often correspond to rapid aqueous-phase reactions which occur within a droplet, and create larger particles with higher concentrations than gas-phase reactions.[40,41] For organic matter, the condensation growth and the oxidation chemical reaction at the particle surface will enlarge particle size during the aerosol aging process.[42]

Our findings in Shanghai indicates that localization of mass scattering efficiencies based on field measurement, especially for locations with high aerosol mass loadings, are necessary to reduce bias of IMPROVE algorithms. Scattering coefficient should be estimated for both polluted episodes and clean conditions due to sharp variation of mass scattering efficiencies at different aerosol mass concentrations which is often accompanied by changing size distriubitons. Further studies are needed for major aerosol absorption species such as black carbon, which is important for both visibility degradation and radiation effect.

AUTHOR INFORMATION

Corresponding Authors

*(J.J.) Phone: +86-10-62781512; fax: +86-10-62773597; e-mail: jiangjk@tsinghua.edu.cn.

*(S.W.) Phone: +86-10-62771466 ; fax: +86-10-62773650; e-mail: shxwang@tsinghua.edu.cn.

Notes

The authors declare no competing financial interest.

ACKNOWLEDGMENTS

This work is supported by the National Natural Science Foundation of China (21107060, 21190054, 41227805, 21422703, and 21221004) and MEP's Special Funds for Research on Public Welfares (201409002, 201409008). We acknowledge Qiang Zhang, Wei Zhou, Jieqiong Liu, Jiandong Wang, Shengrong Lou, and Liping Qiao for their help with the sampling and data analysis.

REFERENCES

(1) Pope, C. A.; Dockery, D. W. Health effects of fine particulate air pollution: Lines that connect. *J. Air Waste Manage. Assoc.* **2006**, *56*, 709−742.

(2) Brunekreef, B.; Holgate, S. T. Air pollution and health. *Lancet* **2002**, *360*, 1233−1242.

(3) Cheng, Z.; Jiang, J.; Fajardo, O.; Wang, S.; Hao, J. Characteristics and health impacts of particulate matter pollution in China (2001−2011). *Atmos. Environ.* **2013**, *65*, 186−194.

(4) Charlson, R. J.; Schwartz, S. E.; Hales, J. M.; Cess, R. D.; Coakley, J. A.; Hansen, J. E.; Hofmann, D. J. Climate forcing by anthropogenic aerosols. *Science* **1992**, *255*, 423−430.

(5) Watson, J. G. Visibility: Science and regulation. *J. Air Waste Manage. Assoc.* **2002**, *52*, 628−713.

(6) Intergovernmental Panel on Climate Change Eds. *Climate Change 2013 − The Physical Science Basis*; Cambridge University Press: Cambridge, 2006.

(7) Bates, T. S.; Anderson, T. L.; Baynard, T.; Bond, T.; Boucher, O.; Carmichael, G.; Clarke, A.; Erlick, C.; Guo, H.; Horowitz, L.; Howell, S.; Kulkarni, S.; Maring, H.; McComiskey, A.; Middlebrook, A.; Noone, K.; O'Dowd, C. D.; Ogren, J.; Penner, J.; Quinn, P. K.; Ravishankara, A. R.; Savoie, D. L.; Schwartz, S. E.; Shinozuka, Y.; Tang, Y.; Weber, R. J.; Wu, Y. Aerosol direct radiative effects over the northwest Atlantic, northwest

DOI: 10.1021/es504567q
Environ. Sci. Technol. 2015, 49, 831−838

Pacific, and North Indian Oceans: Estimates based on in-situ chemical and optical measurements and chemical transport modeling. *Atmos. Chem. Phys.* **2006**, *6*, 1657−1732.
(8) *Spatial and Seasonal Patterns and Temporal Variability of Haze and its Constituents in the United States*; Cooperative Institute for Research in the Atmosphere (CIRA), Colorado State University, 2011; http://vista.cira.colostate.edu/improve/publications/reports/2011/2011.htm.
(9) Hand, J. L.; Malm, W. C. Review of aerosol mass scattering efficiencies from ground-based measurements since 1990. *J. Geophys. Res.* **2007**, *112*, 1−24.
(10) Pitchford, M.; Malm, W.; Schichtel, B.; Kumar, N.; Lowenthal, D.; Hand, J. Revised algorithm for estimating light extinction from IMPROVE particle speciation data. *J. Air Waste Manage. Assoc.* **2007**, *57*, 1326−1336.
(11) *Review of the IMPROVE Equation for Estimating Ambient Light Extinction Coefficients*; Cooperative Institute for Research in the Atmosphere (CIRA), Colorado State University, 2005; http://vista.cira.colostate.edu/improve/publications/graylit/016_IMPROVEeqReview/IMPROVEEquationReview.pdf.
(12) Zhang, G.; Bi, X.; Chan, L. Y.; Wang, X.; Sheng, G.; Fu, J. Size-segregated chemical characteristics of aerosol during haze in an urban area of the Pearl River Delta region, China. *Urban Climate* **2013**, *4*, 74−84.
(13) Tao, J.; Ho, K. F.; Chen, L. G.; Zhu, L. H.; Han, J. L.; Xu, Z. C. Effect of chemical composition of $PM_{2.5}$ on visibility in Guangzhou, China, 2007 spring. *Particuology* **2009**, *7*, 68−75.
(14) Jung, J.; Lee, H.; Kim, Y. J.; Liu, X.; Zhang, Y.; Gu, J.; Fan, S. Aerosol chemistry and the effect of aerosol water content on visibility impairment and radiative forcing in Guangzhou during the 2006 Pearl River Delta campaign. *J. Environ. Manage.* **2009**, *90*, 3231−3244.
(15) Cao, J.; Wang, Q.; Chow, J. C.; Watson, J. G.; Tie, X.; Shen, Z.; Wang, P.; An, Z. Impacts of aerosol compositions on visibility impairment in Xi'an, China. *Atmos. Environ.* **2012**, *59*, 559−566.
(16) Han, S.; Bian, H.; Zhang, Y.; Wu, J.; Wang, Y.; Tie, X.; Li, Y.; Li, X.; Yao, Q. Effect of aerosols on visibility and radiation in spring 2009 in Tianjin, China. *Aerosol Air Qual. Res.* **2012**, *12*, 211−217.
(17) Shen, G.; Xue, M.; Yuan, S.; Zhang, J.; Zhao, Q.; Li, B.; Wu, H.; Ding, A. Chemical compositions and reconstructed light extinction coefficients of particulate matter in a mega-city in the western Yangtze River Delta, China. *Atmos. Environ.* **2014**, *83*, 14−20.
(18) Tao, J.; Zhang, L.; Ho, K.; Zhang, R.; Lin, Z.; Zhang, Z.; Lin, M.; Cao, J.; Liu, S.; Wang, G. Impact of $PM_{2.}5$ chemical compositions on aerosol light scattering in Guangzhou — the largest megacity in South China. *Atmos. Res.* **2014**, *135*−*136*, 48−58.
(19) Zhang, X. Y.; Wang, Y. Q.; Niu, T.; Zhang, X. C.; Gong, S. L.; Zhang, Y. M.; Sun, J. Y. Atmospheric aerosol compositions in China: Spatial/temporal variability, chemical signature, regional haze distribution and comparisons with global aerosols. *Atmos. Chem. Phys.* **2012**, *12*, 779−799.
(20) Jiang, J. K.; Zhou, W.; Cheng, Z.; Wang, S. X.; He, K. B.; Hao, J. M. Particulate matter distributions in China during a winter period with frequent pollution episodes (January 2013) *Aerosol Air. Qual. Res.*, DOI: 10.4209/aaqr.2014.04.0070.
(21) Fu, X.; Wang, S.; Zhao, B.; Xing, J.; Cheng, Z.; Liu, H.; Hao, J. Emission inventory of primary pollutants and chemical speciation in 2010 for the Yangtze River Delta region, China. *Atmos. Environ.* **2013**, *70*, 39−50.
(22) *WHO, Air Quality Guidelines: Global Update 2005: Particulate Matter, Ozone, Nitrogen Dioxide and Sulfur Dioxide*; World Health Organization, 2006; http://www.euro.who.int/data/assets/pdf_file/0005/78638/E90038.pdf?ua=1.
(23) Zhou, M.; Chen, C.; Wang, H.; Huang, C.; Su, L.; Chen, Y.; Li, L.; Qiao, Y.; Chen, M.; Huang, H.; Zhang, G. Chemical characteristics of particulate matters during air pollution episodes in autumn of Shanghai,China. *Acta Sci. Circumstantiae* **2012**, *32*, 81−92.
(24) Zhang, Y. H.; Duan, Y. S.; Gao, S.; Wei, H. P.; Sha, F.; Cai, Y.; Shen, L. P. Characteristics of fine particulate matter during a typical air pollution episode in Shanghai urban area. *China Environ. Sci.* **2011**, *31*, 1115−21.
(25) Liu, J.; Jiang, J.; Zhang, Q.; Deng, J.; Hao, J. A spectrometer for measuring particle size distributions in the range of 3 nm to 10 μm. *Front. Environ. Sci. Eng.* **2014**, 1−10.
(26) Khezri, B.; Mo, H.; Yan, Z.; Chong, S. L.; Heng, A. K.; Webster, R. D. Simultaneous online monitoring of inorganic compounds in aerosols and gases in an industrialized area. *Atmos. Environ.* **2013**, *80*, 352−360.
(27) Bauer, J. J.; Yu, X. Y.; Cary, R.; Laulainen, N.; Berkowitz, C. Characterization of the sunset semi-continuous carbon aerosol analyzer. *J. Air Waste Manage. Assoc.* **2009**, *59*, 826−833.
(28) Marple, V. A.; Rubow, K. L.; Behm, S. M. A microorifice uniform deposit impactor (MOUDI): Description, calibration, and use. *Aerosol Sci. Technol.* **1991**, *14*, 434−446.
(29) Cheng, Z.; Wang, S.; Fu, X.; Watson, J. G.; Jiang, J.; Fu, Q.; Chen, C.; Xu, B.; Yu, J.; Chow, J. C.; Hao, J. Impact of biomass burning on haze pollution in the Yangtze River Delta, China: A case study in summer 2011. *Atmos. Chem. Phys.* **2014**, *14*, 4573−4585.
(30) Chow, J. C.; Watson, J. G.; Lowenthal, D. H.; Magliano, K. L. Size-resolved aerosol chemical concentrations at rural and urban sites in Central California, USA. *Atmos. Res.* **2008**, *90*, 243−252.
(31) Huang, X. F.; He, L. Y.; Xue, L.; Sun, T. L.; Zeng, L. W.; Gong, Z. H.; Hu, M.; Zhu, T. Highly time-resolved chemical characterization of atmospheric fine particles during 2010 Shanghai World Expo. *Atmos. Chem. Phys.* **2012**, *12*, 4897−4907.
(32) Anderson, T. L.; Ogren, J. A. Determining aerosol radiative properties using the TSI 3563 integrating nephelometer. *Aerosol Sci. Technol.* **1998**, *29*, 57−69.
(33) Bohren, C. F., H, D. R. *Absorption and Scattering of Light by Small Particles*; John Wiley & Sons: New York, 1998.
(34) *Matlab Functions for Mie Scattering and Absorption*; Institute of Applied Physics, University of Bern, 2002; http://arrc.ou.edu/~rockee/NRA_2007_website/Mie-scattering-Matlab.pdf.
(35) Quinn, P. K.; Coffman, D. J.; Bates, T. S.; Welton, E. J.; Covert, D. S.; Miller, T. L.; Johnson, J. E.; Maria, S.; Russell, L.; Arimoto, R.; Carrico, C. M.; Rood, M. J.; Anderson, J. Aerosol optical properties measured on board the Ronald H. Brown during ACE-Asia as a function of aerosol chemical composition and source region. *J. Geophys. Res.* **2004**, *109*, D19S01.
(36) Tao, J.; Cao, J.-J.; Zhang, R.-J.; Zhu, L.; Zhang, T.; Shi, S.; Chan, C.-Y. Reconstructed light extinction coefficients using chemical compositions of $PM_{2.5}$ in winter in Urban Guangzhou, China. *Adv. Atmos. Sci.* **2012**, *29*, 359−368.
(37) Ryan, P. A. Improved light extinction reconstruction in interagency monitoring of protected visual environments. *J. Air Waste Manage. Assoc.* **2005**, *55*, 1751−1759.
(38) Sciare, J.; Oikonomou, K.; Cachier, H.; Mihalopoulos, N.; Andreae, M. O.; Maenhaut, W.; Sarda-Esteve, R. Aerosol mass closure and reconstruction of the light scattering coefficient over the Eastern Mediterranean Sea during the MINOS campaign. *Atmos. Chem. Phys.* **2005**, *5*, 2253−2265.
(39) Seinfeld, J. H.; Pandis, S. N. *Atmospheric Chemistry and Physics: From Air Pollution to Climate Change*; John Wiley & Sons: New York, U.S., 2006.
(40) John, W.; Wall, S. M.; Ondo, J. L.; Winklmayr, W. Modes in the size distributions of atmospheric inorganic aerosol. *Atmos. Environ.* **1990**, *24*, 2349−2359.
(41) Hering, S. V.; Friedlander, S. K. Origins of aerosol sulfur size distributions in the Los Angeles basin. *Atmos. Environ.* **1982**, *16*, 2647−2656.
(42) Kavouras, I. G.; Stephanou, E. G. Particle size distribution of organic primary and secondary aerosol constituents in urban, background marine, and forest atmosphere. *J. Geophys. Res.* **2002**, *107*, AAC 7−1−AAC 7−12.

DOI: 10.1021/es504567q
Environ. Sci. Technol. 2015, 49, 831−838